

08/16/2002

## **Superconducting Phase Diagram of Single Crystal MgB<sub>2</sub>**

U. Welp<sup>a</sup>, A. Rydh<sup>a</sup>, G. Karapetrov<sup>a</sup>, W. K. Kwok<sup>a</sup>, G. W. Crabtree<sup>a</sup>, Ch. Marcenat<sup>b</sup>,  
L. Paulius<sup>b</sup>, T. Klein<sup>c</sup>, J. Marcus<sup>c</sup>, K. H. P. Kim<sup>d</sup>, C. U. Jung<sup>d</sup>, H.-S. Lee<sup>d</sup>, B. Kang<sup>d</sup>,  
S.-I. Lee<sup>d</sup>

<sup>a</sup> Materials Science Division, Argonne National Laboratory, Argonne, IL 60439

<sup>b</sup> Département de Recherche Fondamentale sur la Matière Condensée, Service de  
Physique, Magnétisme et Superconductivite, CEA-Grenoble, 38054 Grenoble, France

<sup>c</sup> Laboratoire d'Etude des Proprietes des Solides, CNRS, BP 166, 38042 Grenoble,  
France

<sup>d</sup> NCRICS and Dept. of Physics, Pohang University of Science and Technology, Pohang  
790-784, Republic of Korea

Using magnetization, transport and single-crystal specific heat measurements we have determined the superconducting phase diagram of MgB<sub>2</sub>. A zero-temperature in-plane coherence length of 9.4 nm is found. The superconducting anisotropy  $\gamma$  changes monotonously from a value around 2 near  $T_c$  to above 4.5 near 22 K. We present strong evidence for a surface superconducting state for  $H // c$  which might account for the wide spread in reported values of the superconducting anisotropy.

Keywords: MgB<sub>2</sub> single crystals, upper critical field, surface superconductivity

U. Welp, Materials Science Division, Argonne National Laboratory, 9700 S. Cass  
Avenue, Argonne, IL 60439, USA; (630) 252-7777 (FAX); welp@anl.gov

The remarkably high value of  $T_c = 39$  K in  $\text{MgB}_2$  [1] has sparked renewed interest in the connection between superconducting properties and electronic and structural features of non-copper oxide materials.  $\text{MgB}_2$  is characterized by a complex Fermi surface consisting of disconnected sections: a three dimensional tubular network of mostly boron  $\pi$ -states and two dimensional cylindrical sheets derived mostly from boron  $\sigma$ -states [2,3]. The electron-phonon coupling is found to be very anisotropic [4] being the strongest between the 2D-electrons and boron-breathing modes. As a consequence,  $\text{MgB}_2$  is the first example of a superconductor containing two distinct superconducting gaps, a large gap on the 2D Fermi surface sheets and a small, largely proximity induced gap on the 3D sheets [5,6]. The manifestation of this electronic structure in macroscopic quantities such as the superconducting critical fields and the anisotropy parameter  $\gamma = H_{c2}^{ab}/H_{c2}^c = \xi_{ab}/\xi_c$  has attracted much attention. Here,  $H_{c2}^{ab}$ ,  $H_{c2}^c$ ,  $\xi_{ab}$ ,  $\xi_c$  are the in-plane and out-of-plane upper critical fields and Ginsburg-Landau coherence lengths, respectively. However, reported values of the anisotropy coefficient in particular, vary widely ranging from 1.1 to 6 depending on the measurement technique and on sample type, i.e. single crystals [7-12,17,20], oriented films [13], aligned crystallites [14], or powders [15,16]. Recent torque [11], thermal conductivity [12] and magnetization [15-17] measurements indicate that the anisotropy coefficient is temperature dependent, increasing strongly with decreasing temperature.

Here we present a determination of the upper critical field and its anisotropy using magnetization  $M(T)$ , magneto-transport, and single-crystal specific heat  $C_p(T)$  measurements. The transport and magnetization data were taken on the same crystals. A zero-temperature GL coherence length of  $\xi_{ab}(0) = 9.4$  nm is obtained. Transport data

reveal a pronounced peak-effect in the critical current density at  $H_{c2}^c$ . Non-ohmic transport behavior and sharp features in the angular dependence of the resistivity are indicative for the appearance of surface superconductivity. Upward curvature in  $H_{c2}^{ab}(T)$  results in a temperature dependent anisotropy that increases from about 2 near  $T_c$  to above 4.5 at 22 K. We note that the occurrence of surface superconductivity could account for the wide variation in reported values for the anisotropy constant.

The MgB<sub>2</sub> crystals were prepared through a high-pressure synthesis [18]. The crystals are well shaped with straight hexagonal facets and smooth faces (see insets of Fig. 1a) with typical size of 50 μm. The magnetization was measured in a commercial SQUID magnetometer, and the specific heat was measured in an ac-specific heat calorimeter [19] optimized to detect signals from minute crystals (on the order of 50 ng).

Fig. 1a shows the temperature dependence of the resistance measured on cooling in zero field. The sample is characterized by a residual resistivity ratio  $RRR = R(290K)/R(40K) \approx 3.5$  and a resistivity at 40 K of  $\rho = 1.6 \mu\Omega\text{cm}$ . These parameter values are typical for MgB<sub>2</sub> crystals [7-10]. From the resistivity data in Fig. 1a and the Drude relation  $l = 3/[\rho N(0)v_F e^2]$  a rather long electron mean free path of  $l \approx 100$  nm can be estimated using the density of states  $N(0) = 0.7/(\text{eV unit cell})$  [5] and in-plane Fermi velocity  $v_F = 4.8 \cdot 10^7$  cm/sec [2]. The evolution of the superconducting transition in fields applied parallel to the c-axis and to the ab-plane is shown in Figs. 1 b and 1c. For increasing field along c the resistive transition broadens significantly. Similar broadening has been observed in previous studies on single crystals [8,9]. However, here we show that the broadening is strongly current dependent. Non-ohmic behavior appears at the onset of the transition, labeled  $T_{\text{on}}$ . With increasing current a steep resistive drop emerges at a lower temperature

labeled  $T_p$ . In a certain field range around 1.5 T non-monotonous resistivity behavior arises that is reminiscent of the peak-effect [20]. For fields applied along the  $ab$ -directions the resistive transitions in magnetic fields do not broaden (see Fig. 1c) in agreement with previous reports [8,9], and the peak-effect is largely suppressed in the present field and temperature range. The peak-effect in  $\text{MgB}_2$  will be discussed in more detail elsewhere [20,21].

Figures 2a and 2b show the temperature dependence of the magnetization measured on warming after field cooling the sample for  $H \parallel c$  and  $H \parallel ab$ , respectively. Breaks in the slope of  $M(T)$  indicated by the vertical dotted lines are clearly seen and mark the onset of superconductivity. With increasing field there is an essentially parallel shift of the superconducting transition to lower temperatures. This shift is much more pronounced for  $H \parallel c$  indicating a strong superconducting anisotropy of  $\text{MgB}_2$  as discussed below.

The temperature dependence of the specific heat in various fields applied along the  $c$ -axis is shown in Fig. 3. The data are shown as  $C/T$  relative to the data in 3 T, a field which suppresses the superconducting transition well below the covered temperature range. In zero field a clear step with a width of about 2 K is observed. With increasing field the step stays well defined and the step height decreases as expected. However, in contrast to results on polycrystalline samples [5], the width remains essentially constant. Defining  $T_c$  using an entropy conserving construction a phase boundary is obtained that agrees with that determined from  $M(T)$  as discussed below. Thus, the data shown in Figs. 2 and 3 represent the thermodynamic bulk transition of  $\text{MgB}_2$  into the superconducting state. The magnetic, calorimetric and transport data are summarized in the phase diagram shown in Fig. 4. For  $H \parallel c$  the onsets of superconductivity as determined  $M(T)$  and  $C_p(T)$

coincide with each other and with the location of the peak effect within the experimental uncertainty. We identify this line with the upper critical field for the c-axis,  $H_{c_2}^c(T)$ . A zero-temperature value of  $H_{c_2}^c(0) \approx 3.5$  T can be estimated which, using the relation  $H_{c_2}^c(0) = \Phi_0/2\pi\xi_{ab}^2(0)$ , yields the zero-temperature coherence length  $\xi_{ab}^2(0) \approx 9.4$  nm. This length is significantly shorter than the electron mean free path,  $l \approx 100$  nm, indicating that MgB<sub>2</sub> is a superconductor in the clean limit.

For  $H \parallel ab$  determinations of  $T_c(H)$  based on the break in  $M(T)$  and on the resistive onsets coincide within the experimental uncertainty, yielding the  $H_{c_2}^{ab}$ -line shown in Fig. 4. While the upper critical field for  $H \parallel c$  follows a conventional temperature dependence, a pronounced upward curvature of  $H_{c_2}$  was observed for the ab-directions. As a result the superconducting anisotropy is temperature dependent as shown in the inset of Fig. 4 increasing from about 1.5 to 2 near  $T_c$  to above 4.5 at 22 K. Similar results have recently been obtained from torque [11], magnetization [16,17] and thermal conductivity [12] measurements.

An upward curvature of the  $H_{c_2}$ -line near  $T_c$  and a temperature dependent anisotropy have been observed in layered superconductors including NbSe<sub>2</sub> [22] and borocarbides [23,24]. These effects can have several origins [25], including anisotropy of the Fermi surface, of the pairing potential and of the superconducting gap, and they are generally most pronounced in clean materials where, due to non-local effects, Fermi surface anisotropies and gap anisotropies affect macroscopic quantities such as the upper critical field. In dirty materials strong impurity scattering washes the anisotropies out. An upward curvature of the  $H_{c_2}$ -line near  $T_c$  and a temperature dependent anisotropy can not be accounted for in standard Ginzburg-Landau theory incorporating effective mass

anisotropy only. They have been addressed in various theoretical approaches including non-local corrections and gap anisotropies [26], two (multi)-band models [24,27,28,29], strong-coupling calculations with realistic band structures [30]. A two-band approach seems appropriate for MgB<sub>2</sub> [28,29] since its electron system naturally falls into two groups. At low temperatures / high fields the upper critical field is dominated by the highly anisotropic 2D-bands (the 3D-gap being largely suppressed in high fields [5,6]) resulting in the large measured values of the anisotropy. At high temperatures, while approaching  $T_c$ , the superconducting transition involves the entire Fermi surface, including the 3D-band, resulting in a reduced anisotropy between 1.5 and 2.

Also included in the phase diagram, Fig. 4, is a line defined by the onset of non-ohmic transport at  $T_{on}$  (see Fig. 1b). This line lies by a factor of about 1.7 above the  $H_{c2}$ -line suggesting that the resistive onset is a manifestation of surface superconductivity [31] at  $H_{c3}$  which for a flat surface in parallel magnetic field occurs at  $1.7 \times H_{c2}$ . Although resistive transitions as shown in Fig. 1b could in principle result from filamentary conduction along impurity phases the observation of a single sharp, current-independent superconducting transition in zero field indicates an intrinsic mechanism. In addition, nearly identical resistivity results were obtained on a second, smaller crystal. We also note that the limits of the resistive broadening reported earlier [8] encompass the same coefficient, 1.7. Furthermore, non-ohmic transport data above the bulk upper critical field have been reported for NbTa and PbIn samples [32] and for NbSe<sub>2</sub> crystals [33]. These results, closely resembling those in Fig. 1b, have been interpreted as signature of surface superconductivity.

The angular dependence of the resistivity of a third crystal measured in the regime of non-ohmic transport above the bulk upper critical field is shown in Fig. 5. Pronounced cusp-like dips in the resistance with a width of about  $5^\circ$  are observed when the field is aligned with the  $c$ -axis. With increasing angle  $\Theta$  the resistance increases rapidly and at high angles decreases again due to the superconducting anisotropy of  $\text{MgB}_2$ . This kind of angular dependence could be caused by extended crystal defects containing the  $c$ -axis such as small angle grain boundaries or a high density of edge dislocations with cores parallel to  $c$ . Extensive microstructural studies [34] on sintered polycrystalline  $\text{MgB}_2$ -samples have revealed as a common defect edge dislocations with cores parallel to the  $ab$ -planes. These, however, would not account for the observed transport behavior. In addition, x-ray diffraction reveals a very high quality of the crystals without any indication for small angle grain boundaries [18]. Furthermore, the dip is strongly dependent on the azimuthal angle being most pronounced when the field rotates in a plane perpendicular to the side face ( $\Phi = 60^\circ$ ) and being largely suppressed for rotation in the plane of the side face ( $\Phi = -30^\circ$ ). These results are consistent with a surface superconducting state which is rapidly suppressed by magnetic field components perpendicular to the surface [35].

Since surface superconductivity does not contribute to the magnetization [31] nor to the thermal conductivity of macroscopic samples but does induce non-linear response in the resistivity, a discrepancy between both determinations might be expected. In fact, reported  $\gamma$ -values determined from resistivity measurements (usually the resistive onset is identified with  $H_{c2}$  on crystals [7-10] as well as on  $c$ -axis oriented films [13] are generally low, in the range of 2 to 3. In contrast, magnetic measurements on either powder samples

[15,16] or on single crystals [11,17] as well as thermal conductivity measurements [12] yield  $\gamma$ -values around 6 at low temperatures.

In conclusion, the superconducting phase diagram of  $\text{MgB}_2$  has been determined using magnetization, magneto-transport and single-crystal specific heat measurements. The in-plane coherence length is 9.4 nm corresponding to  $H_{c2}^c(0) \approx 3.5$  T. The superconducting anisotropy increases with decreasing temperature from a value around 2 near  $T_c$  to above 4.5 at 22 K. For  $H \parallel c$  a pronounced peak effect in the critical current occurs at the upper critical field. Evidence for a surface superconducting state is presented for  $H \parallel c$  which might account for the wide spread of reported for the anisotropy coefficient.

This work was supported by the U.S. Department of Energy, BES, Materials Science under contract W-31-109-ENG-38, by the National Science Foundation under grant No.0072880, the Fulbright Program (A.R.), and by the Ministry of Science and Technology of Korea through the Creative Research Initiative Program.

## References

- [1] J. Nagamatsu et al., Nature **410** (2001), 63.
- [2] J. M. An, W. E. Pickett, Phys. Rev. Lett. **86** (2001), 4366; J. Kortus et al., Phys. Rev. Lett. **86** (2001), 4656.
- [3] E. A. Yelland et al., Phys. Rev. Lett. **88** (2002), 217002.
- [4] H. J. Choi et al., cond-mat/0111182; *ibid* cond-mat/0111183; T. Yildirim et al., Phys. Rev. Lett. **87** (2001), 037001; R. Osborn et al., Phys. Rev. Lett. **87** (2001), 017005.
- [5] F. Bouquet et al., Phys. Rev. Lett. **87** (2001), 047001; Y. Wang et al., Physica C **355** (2001), 179.
- [6] P. Szabo et al., Phys. Rev. Lett. **87** (2001), 137005; F. Giubileo et al., Phys. Rev. Lett. **87** (2001), 177008; X. K. Chen et al., Phys. Rev. Lett. **87** (2001), 157002; H. Schmidt et al., Phys. Rev. Lett. **88** (2002), 127002; M. Iavarone et al., cond-mat/0203329.
- [7] K. H. P. Kim et al., Phys. Rev. B **65** (2002), 100510.
- [8] S. Lee et al., J. Phys. Soc. Jpn. **70** (2001), 2255; Yu. Eltsev et al., cond-mat/0202133; Phys. Rev. B **65** (2002), 140501.
- [9] A. K. Pradhan et al., Phys. Rev. B **64** (2001), 212509.
- [10] M. Xu et al., Appl. Phys. Lett. **79** (2001), 2779.
- [11] M. Angst et al., Phys. Rev. Lett. **88** (2002), 167004.
- [12] A. V. Sologubenko et al., Phys. Rev. B **65** (2002), 180505.
- [13] S. Patnaik et al., Supercond. Sci. Techn. **14** (2001), 315; M. H. Jung et al., Chem. Phys. Lett. **343** (2001), 447; R. J. Olsson et al., cond-mat/0201022.

- [14] O. F. de Lima et al. Phys. Rev. Lett. **86** (2001), 5974.
- [15] F. Simon et al., Phys. Rev. Lett. **87** (2001), 047002; S. L. Bud'ko et al., Phys. Rev. B **64** (2001), 180506.
- [16] S. L. Bud'ko et al., cond-mat/0201085.
- [17] M. Zehetmayer et al., cond-mat/0204199.
- [18] C. U. Jung et al., cond-mat/0203123.
- [19] F. Bouquet et al., Nature **411** (2001) 488.
- [20] U. Welp et al., cond-mat /0203337.
- [21] A. Rydh et al., to be published.
- [22] Y. Muto et al., Physics Letters **45 A** (1973), 99; J. A. Woollam et al., Phys. Rev. Lett. **32** (1974), 712.
- [23] V. Metlushko et al., Phys. Rev. Lett. **79** (1997), 1738.
- [24] S. V. Shulga et al., Phys. Rev. Lett. **80** (1998), 1730.
- [25] for early reviews see: “Anisotropy effects in Superconductors” , ed. H. W. Weber (Plenum Press, New York, 1977).
- [26] K. Takanaka, Phys. Stat. Solidi B **68** (1975), 623; H. Teichler, Phys. Stat. Solidi B **69** (1975), 501.
- [27] P. Entel, M. Peter, J. Low. Temp. Phys. **22** (1976), 613.
- [28] P. Miranovic et al., cond-mat/0207146.
- [29] G. Fuchs et al., in “Studies of High Temperature Superconductors” ed. A. Narlikar (Nova Science Publishers, New York, 2002), Vol. 41, p. 171.
- [30] M. Prohammer, E. Schachinger, Phys. Rev. B **36** (1987); E. Langmann, Phys. Rev. B **46** (1992) 9104; and references therein.

- [31] D. Saint-James and P. G. de Gennes, *Phys. Lett.* **7** (1963), 306; A. A. Abrikosov, *Sov. Phys.-JETP* **20** (1965), 480.
- [32] C. F. Hempstead, Y. B. Kim, *Phys. Rev. Lett.* **12** (1964), 145.
- [33] G. D'Anna et al., *Phys. Rev. B* **54** (1996), 6583.
- [34] Y. Zhu et al., *Physica C* **356** (2001), 239.
- [35] R. S. Thompson, *Sov. Phys.-JETP* **42** (1976), 1144.

## Figure captions

Fig.1 a) Temperature dependence of the resistance in zero field measured on cooling between room temperature and 30 K. The insets show photos of the crystals, the lower right being the crystal used for the angular dependent measurements (see Fig. 5).

b) Temperature dependence of the resistance measured in various magnetic fields along the *c*-axis with measuring currents of 1 mA (broken lines) and 10 mA (solid lines).  $T_{on}$  and  $T_p$  mark the onset of non-ohmic transport behavior and the sudden drop to zero resistance seen at high currents, respectively.

c) Temperature dependence of the resistance measured in various magnetic fields along the *ab*-axes.

Fig. 2 Temperature dependence of the magnetization measured on warming after cooling the sample in the indicated fields along the *c*-axis (a) and along the *ab*-axes (b).

Fig. 3 Temperature dependence of  $C/T$  in various fields applied along the *c*-axis. Between 0 and 1 T data were taken every 0.1 T. The data are normalized to those in a field of 3 T.

Fig. 4 Superconducting phase diagram of single crystal  $\text{MgB}_2$ . Included are data derived from the resistive onsets for fields along the *c*- and *ab*-axes, from the onset of diamagnetism for both field orientations, from the specific heat measured for  $H //$

$c$ , and from the resistive drop at  $T_p$  (see Fig. 1b) labeled “peak” in the phase diagram. The inset shows the temperature dependence of the anisotropy coefficient  $\gamma$ .

Fig. 5 Angular dependence of the resistance measured around the  $c$ -axis for various azimuthal angles. The inset defines the geometry.

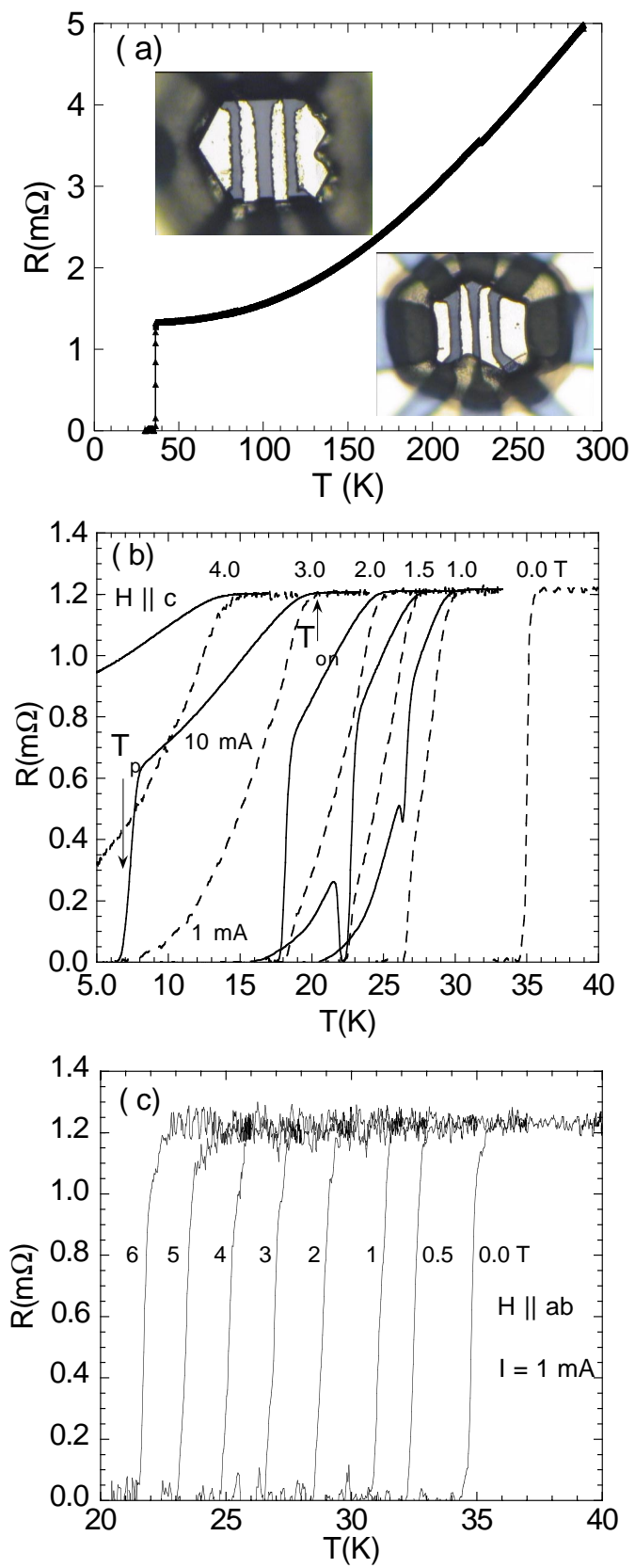


Fig.1  
U. Welp et al.

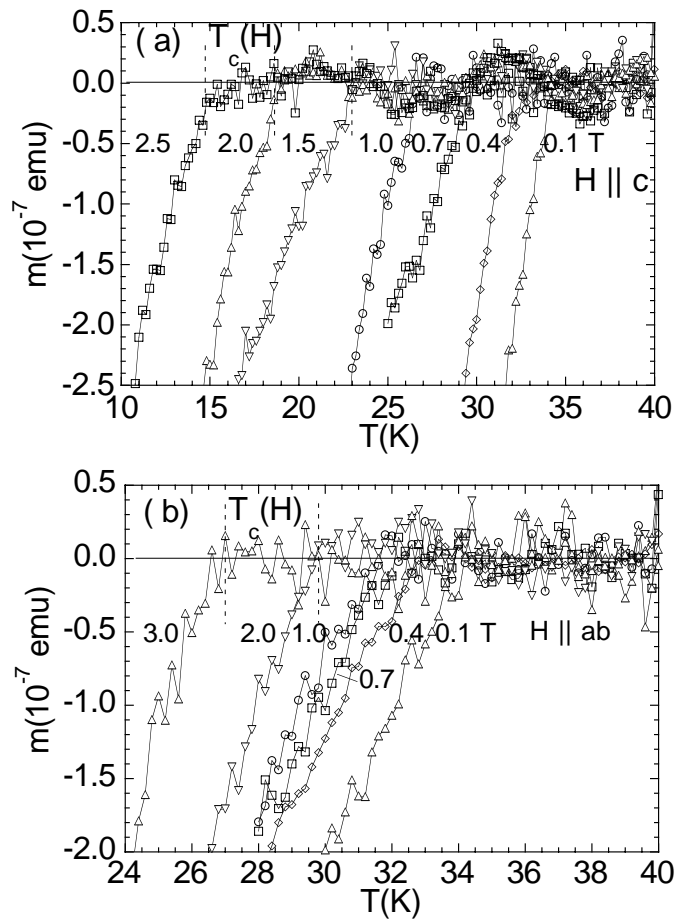


Fig. 2  
U. Welp et al.

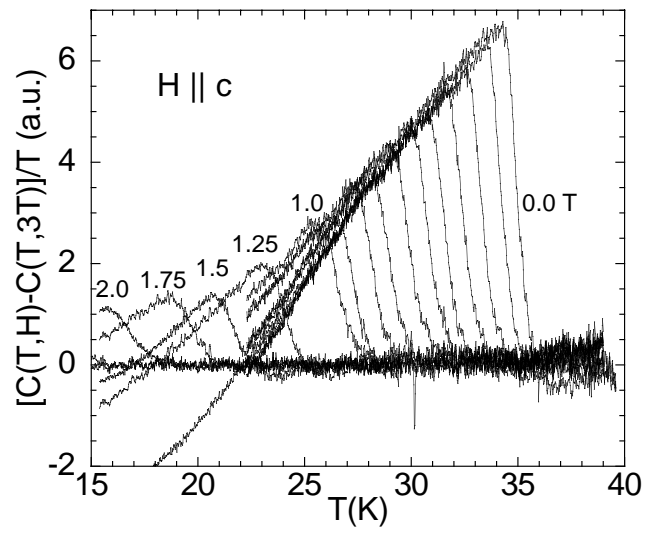


Fig. 3  
U. Welp et al.

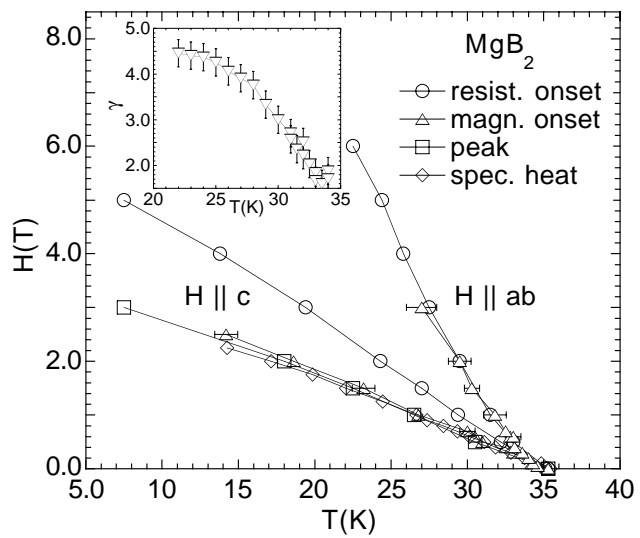


Fig. 4  
U. Welp et al.

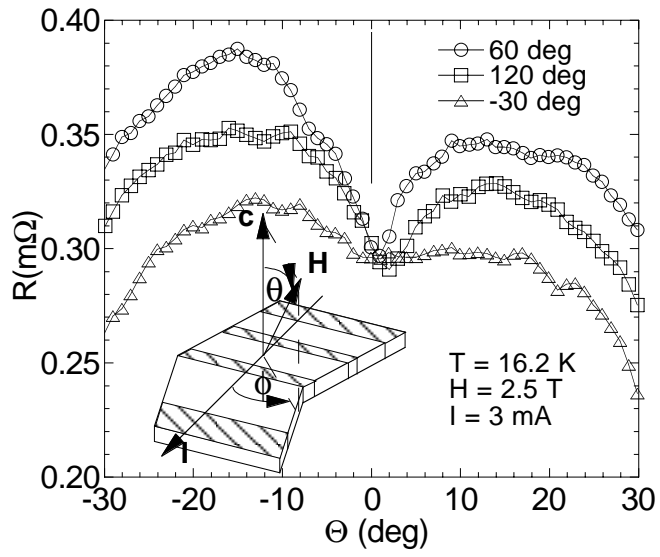


Fig. 5  
U. Welp et al.